Multilayer Volume Holographic Optical Memory

Vladimir Markov, James Millerd, James Trolinger, Mark Norrie

MetroLaser Inc., Suite 100, Skypark Circle 18010, Irvine, California 92614

John Downie*, Dogan Timucin*

*NASA Ames Research Center, M/S 269-3, Moffett Field, CA 94035

We demonstrate a scheme for volume holographic storage based on the features of shift selectivity of a speckle reference wave hologram. The proposed recording method allows more efficient use of the recording medium and increases the storage density in comparison with spherical or plane-wave reference beams. Experimental results of multiple hologram storage and replay in a photorefractive crystal of iron-doped lithium niobate are presented. The mechanism of lateral and longitudinal shift selectivity are described theoretically and shown to agree with experimental measurements.

Holographic memory has been a subject of interest for decades since it was first suggested by van Heerden [1]. High information density, parallel access and high-speed retrieval are among the features that make this technique of data storage so attractive. Selective properties of volume holograms due to angular [2,3] or wavelength deviation [4] from the Bragg condition, as well as reference beam phase encoding [5] are the methods frequently used for data input and retrieval. The combination of reference beam phase encoding with spatial-shift multiplexing was shown to be an efficient approach for high-density holographic information storage [6,7]. A similar technique using a reference beam comprised of many plane waves (or a spherical wave) was suggested and experimentally demonstrated [8]. Although all these methods allow storing the holograms with high density, the longitudinal shift component of the volume recording media has not been considered for coding the individual "pages" of information. Recently, the method of multilayer optical storage was discussed in which information is recorded at different depths within the media, similar to that of a magnetic disc stack currently used in PC's.[9,10] It was demonstrated that holograms can be recorded as thin layers within the volume of the medium to provide high information storage capacity

29 and fast data transfer rates.[11] In this Letter we discuss and demonstrate a single volume, multilayer
30 holographic optical memory, based on the features of 3D spatial-shift selectivity in a volume
31 hologram recorded with a speckle-encoded reference beam (**SRB**).

32 For our analysis, we consider the case where the hologram is recorded by a plane wave signal
33 beam $\mathbf{S_o(r)}$ and a **SRB** $\mathbf{R_o(r)}$ with a divergence angle $\delta\theta_{SP}$, as shown on Fig.1. The two recording
34 beams intersect at an angle θ_o forming the interference pattern with a grating spacing $\Lambda = \lambda/sin(\theta_o)$,
35 assuming a **SRB** incidence angle $\theta_{Ro} = 0$. It was shown [12] that in the first Born approximation, the
36 diffracted wave amplitude **S(r)**, when reconstructed with **SRB** different from the recording one **(i.e.**
37 $\mathbf{R(r) \neq R_o(r))}$, can be described as:

38
$$S(r) = k_o^2 \iiint_V \delta\varepsilon(r')R(r')\frac{\exp[ik_o(r-r')]}{4\pi|r-r'|}d^3r'. \qquad (1)$$

39 Here $\delta\varepsilon(r')$ is the modulated component of the recording media permittivity $\delta\varepsilon(r) \propto S_O(r)R_O^*(r)$ and
40 **V** is the volume of the hologram. Eq.(1) is valid if the hologram is volume and its thickness **T**
41 exceeds the longitudinal speckle size, i.e. $\mathbf{T} >> \lambda/(\delta\theta_{SP})^2 >> \lambda/2\theta_o$. Then, by assuming a plane wave
42 signal beam $\mathbf{S_o(r)} = \exp(i\mathbf{k_{os}r})$ and reconstructed signal beam **S(r)** propagating in the same direction,
43 Eq. (1) can be reduced to

44
$$S(r) = \exp(ik_{os}r)\iiint_V C(r,r')d^3r'. \qquad (2)$$

45 It is assumed here that the speckle pattern intensity distribution has Gaussian statistics and its' spatial
46 auto-correlation function $\mathbf{C(r,r')}$ is determined by mutual intensity of the recording and
47 reconstructing **SRB** [13], i.e. $\mathbf{C(r,r')} = \langle R_o^*(r)R(r')\rangle$.

48 Contrary to the usual practice for a phase-encoded holographic memory, we consider the case

when the spatial amplitude-phase distribution of the reconstruction beam **R(r)** remains identical to that of the recording one $\mathbf{R_o(r)}$. The difference between **R(r)** and $\mathbf{R_o(r)}$ is due to mutual spatial shift of the hologram and reconstructing beam, i.e. $\mathbf{R(r)} = \mathbf{R_o(r + \vec{\Delta})}$, here $\vec{\Delta} = \Delta_\perp \hat{q} + \Delta_{II}\hat{z}$; $\Delta_\perp$, Δ_{II} are transverse and longitudinal components of the shift, and $\hat{q}, \hat{z}$ are unity vectors in the same directions.

As the experimentally measured value is the diffracted beam intensity $\mathbf{I_D} = |S|^2$, it is convenient to introduce the parameter of relative diffracted beam intensity $\mathbf{I_{DN}(\Delta)} = \mathbf{I_D(\Delta)/I_{D(\Delta=0)}}$, where the measured diffracted intensity $\mathbf{I_D(\Delta)}$ is normalized by its peak value at zero shift $\mathbf{I_{D(\Delta=0)}}$. By incorporating the three-dimensional correlation function **C(r, r')** derived in [12] and using the Fresnel-Kirchhoff diffraction integral, the dependence $\mathbf{I_{DN}}(\vec{\Delta}_\perp)$ can be expressed as:

$$I_{DN}(\Delta_\perp) = \frac{I_D(\Delta_\perp)}{I_{D(\Delta_\perp=0)}} = \frac{\left| \int_0^T \exp\left[\frac{ik_o n \Delta_\perp^2}{2d_{dh}} \right] \int_{-\infty}^{+\infty} \int |K_D(\vec{q})|^2 \times \exp\left[-\frac{ik_o n}{d_{dh}} \vec{q}\vec{\Delta}_\perp \right] d^2q dz \right|^2}{T^2 \times \int_{-\infty}^{+\infty} \int |K_D(\vec{q})|^2 d^2q,} \quad (3)$$

Here, $K_D(\vec{q})$ is the diffuser aperture function, $k_o = 2\pi/\lambda$; $\vec{q} = q_x\vec{x} + q_y\vec{y}$, **n** is refraction index of the recording media, and $\mathbf{d_{dh}}$ is the diffuser-hologram distance.

It follows from Eq. 3 that any lateral mismatch between the hologram and the reconstruction beam **R(r)** leads to a decrease of the diffracted beam intensity. Fig.2 shows the fall-off in $\mathbf{I_{DN}(\Delta)}$ that occurs for lateral shift (Δ_{II} = const). One of the important feature of this type of selectivity is that no ripples are observed as a function of spatial mismatch, unlike in case of angular or spectral selectivity of volume holograms recorded with plane or spherical waves. The monotonic decrease in diffraction efficiency as a function of shift distance results in a much lower crosstalk between stored images than can be obtained using other forms of multiplexing. Furthermore, the spatial de-correlation is

symmetric within the plane perpendicular to Z-direction whereas other forms of multiplexing have high selectivity only in the dispersion plane.

Since the speckle pattern has a three-dimensional nature, the longitudinal shift also results in spatial de-correlation between the hologram and reconstructing speckle-beam and thus a third dimension can be used to multiplex information. It can be shown that analogously to $I_{DN}(\Delta_\perp)$ the diffracted beam intensity $I_{DN}(\Delta_{II}) \rightarrow 0$, when the shift distance Δ_{II} exceeds the longitudinal correlation length $<\sigma_{II}>$ (see Fig.2). This opens the possibility to implement several "*virtual layers*" of holograms within the same volume of the recording media.

SRB holograms were recorded in 2.8-mm-thick Fe:$LiNbO_3$ (0.02% Fe/mol) crystal using 3D-shift multiplexing. The crystal, with its *C*-axis laying in plane of the recording beams, was set onto an XYZ computer controlled positioning table, which had a precision 0.025 μm in X, Y, and Z planes. A 1 cm diameter CW argon laser beam ($\lambda = 515$ nm, $P = 40$ mW/cm^2) was used as the coherent light source for hologram recording. The **SRB** had a lateral speckle size $<\sigma_\perp> \approx 3$ μm and intersected with the plane wave signal beam at an angle of $\theta_o = 35°$ ($\theta_{Ro} = 0°$ and $\theta_{So} = 35°$). The diffracted beam intensity was measured using a pin photo-detector.

The diffraction efficiency of the hologram in its' original position ($\Delta = 0$) was approximately 10^{-3}. After each hologram was recorded a lateral shift $\Delta_\perp = 10$ μm was introduced to record the next page of information. The raster scan sequence was used to multiplex images in X, Y and Z as shown in Fig.1. During reconstruction, proper mutual re-positioning of the hologram and the **SRB** resulted in information retrieval. A typical sequence of 30 holograms stored in the form of a 6×5-matrix is shown in Fig.3. The scan step-length for this matrix reconstruction was 0.25 μm. Notice the symmetric nature of the selectivity in both X and Y directions that is characteristic of using a **SRB**.

Once recording of the first layer $\mathbf{L_1}$ was completed, the next layer $\mathbf{L_i}$ was formed by shifting the recording media (or diffuser that generated the speckle pattern) along the central axis of the speckle beam propagation. The shift magnitude, as discussed before, should satisfy the condition $\Delta_{II} \geq \langle\sigma_{II}\rangle$, which for our experimental set up was about 30 μm. In this way, the new layer $\mathbf{L_2}$ could be recorded with the same lateral shift selectivity and thus a new matrix of $n_{L2} \times m_{L2}$ holographic "pages" was formed. The effect of longitudinal shift selectivity was measured for two holograms and is shown in Figure. A longitudinal shift (Z direction) of $\Delta_{II} = 40$ μm was introduced between each recording. Figure 4 also shows an example of the diffracted signal reconstructed from a two-layer structure, in which each layer is composed from a matrix of 4 x 3.

We now estimate the storage density for the above-described technique of holographic data multiplexing. The number of the holograms $\mathbf{N_\perp}$ to be recorded in one layer can be calculated as the ratio between an effective area $\mathbf{F}$ of the recording media and unitary lateral shift area $(\Delta_\perp)^2$ in this plane, i.e. $\mathbf{N_\perp} \approx (l_x \times l_y)/(\Delta_\perp)^2$, where l_x, l_y are lateral dimensions of the recording media. The number of the available layers is proportional to $\mathbf{T}/\Delta_{II}$. The total number of the holograms that can be recorded with shift selectivity scheme can be estimated as $\mathbf{N_{SP}} = \mathbf{V}/[(\Delta_\perp)^2 \times \Delta_{II}]$. This leads to $\mathbf{N_{SP}} \sim 4\times10^9$ holograms for $1\times1\times1\text{cm}^3$ crystal, for above described experimental conditions ($\langle\sigma_\perp\rangle \approx 3$ μm, $\langle\sigma_{II}\rangle \approx 30$ μm). In a practical system, the maximum storage density is further limited by the dynamic range of the refraction index variation and the signal-to-noise ratio (SNR) of the reconstructed image. The average SNR for each of the holograms reconstructed in these experiments was ≤ 45. It was measured as the ratio between the Fourier-filtered DC component of the diffracted beam and the collected scattered light that propagates in the same direction. At fixed experimental conditions, such as recording beam ratio, exposure level, form of the aperture in diffuser plane, etc.,

112 the value of SNR depends upon the ratio between introduced shift $\Delta_{\perp,\parallel}$ and the magnitude of the
113 correlation radius $<\sigma_{\perp,\parallel}>$ in corresponding direction.

114 In conclusion, we have demonstrated the possibility to create a "multilayer" holographic
115 memory in a photorefractive crystal based on the 3D spatial shift selectivity of speckle-encoded
116 reference waves. The method achieves high-density data storage with a simple storage-retrieval
117 architecture.

118 This research was supported in part by the NASA Ames Research Center. The authors thank
119 Michael Dang for technical assistance.

120

121

122

123

124

125

126

127

128

129

130

131

132

133

134

References

1. P. Van Heerden, Appl.Opt. **2**, 156 (1963)
2. F. H. Mok, Opt. Lett. **18**, 915 (1993)
3. S. Tao, D. Selvian, J. Midwinter, Opt.Lett. **18**, 912 (1993)
4. J. Rosen, Opt.Lett. **18**, 744 (1993)
5. G. Rakuljc, Opt.Lett. **17**, 1471 (1992)
6. A. Darskii, V. Markov, SPIE Proc. **1600**, 318 (1992)
7. V. Markov Yu. Denisyuk, R. Amezquita, Opt. Mem. Neural Networks **6**, 91 (1997)
8. D. Psaltis, M. Leven, A. Pu, et all, Opt. Lett. **20**, 782 (1995)
9. J. Rosen, SPIE Proc. **2514**, 14 (1995)
10. S. Chinn, E. Swanson, Opt. Lett. **21**, 899 (1996)
11. P. Mitkas, L. Irakliotis, Opt. Mem. Neural Networks **3**, 217 (1994)
12. A. Darskii, V. Markov, Opt.&Spectrosc., **65**, 661 (1988)
13. L. Laushacke, M. Kirchner, J.Opt. Soc. Am. **A7**, 827 (1990)

158

159

160

Figure captions

161 Fig. 1. The scheme of multilayer speckle-reference beam encoded hologram recording.

162 Fig. 2. Calculated diffracted beam intensity $\mathbf{I_N}(\Delta)$ as a function of lateral $\Delta_\perp$ and longitudinal $\Delta_{||}$ shift

163 at hologram reconstruction with speckle-encoded reference beam.

164 Fig. 3. Measured diffraction efficiency of 30 holograms multiplexed with lateral shift $\Delta_\perp$ = 10 μm

165 between each recording.

166 Fig. 4. Measured diffracted beam intensity as a function of spatial shift in X,Y and Z directions for

167 two holographic recordings having a longitudinal shift of 30 μm between each Z-shift, and two-layer

168 holographic memory structure, each layer composed by the matrix of 4 x 3 holograms.

169

170

171

172

173

174

175

176

177

178

179

180

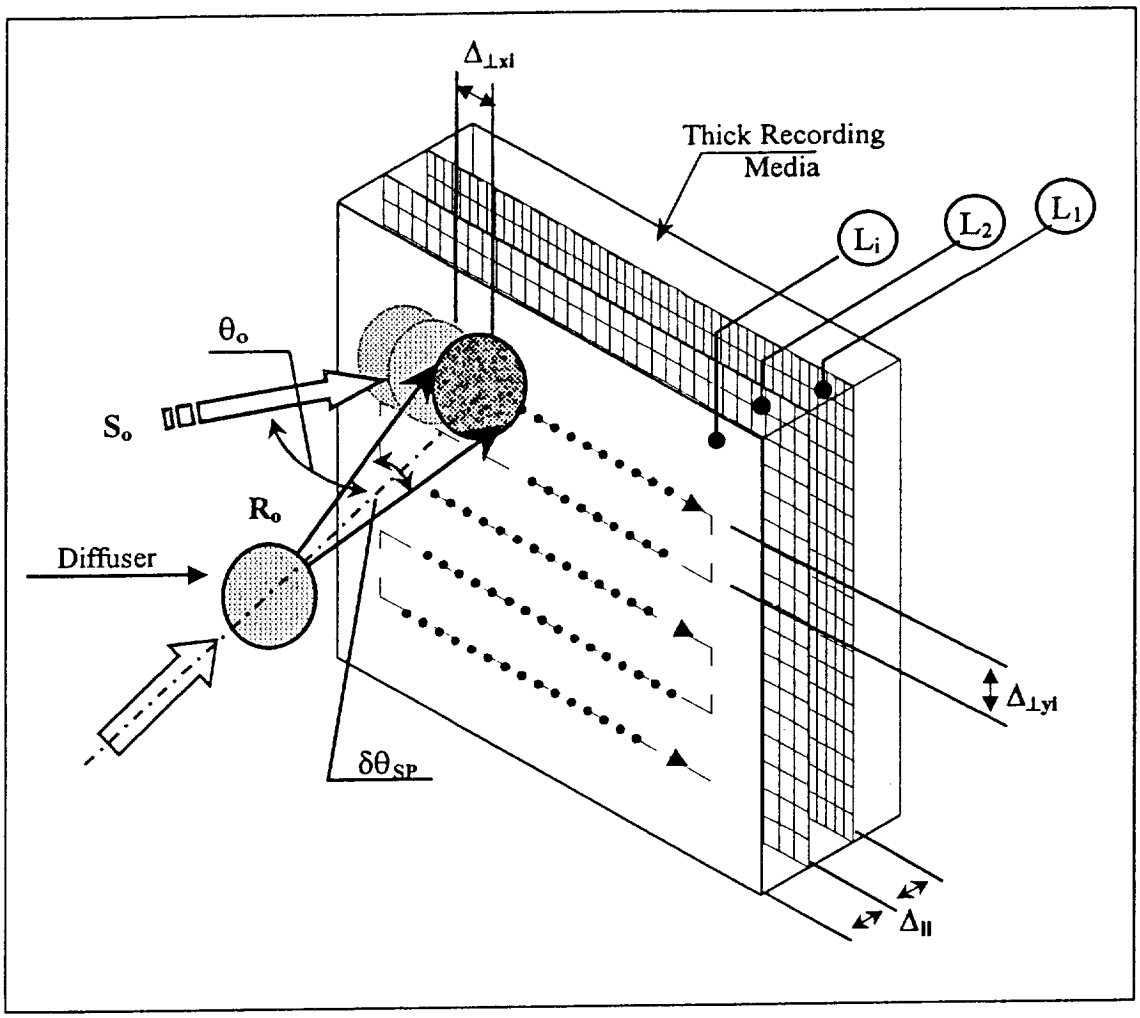
$\Delta_{\perp xi}$
Thick Recording Media
L_i
L_2
L_1
θ_o
S_o
R_o
Diffuser
$\delta\theta_{SP}$
$\Delta_{\perp yi}$
$\Delta_{\parallel}$

Fig.1

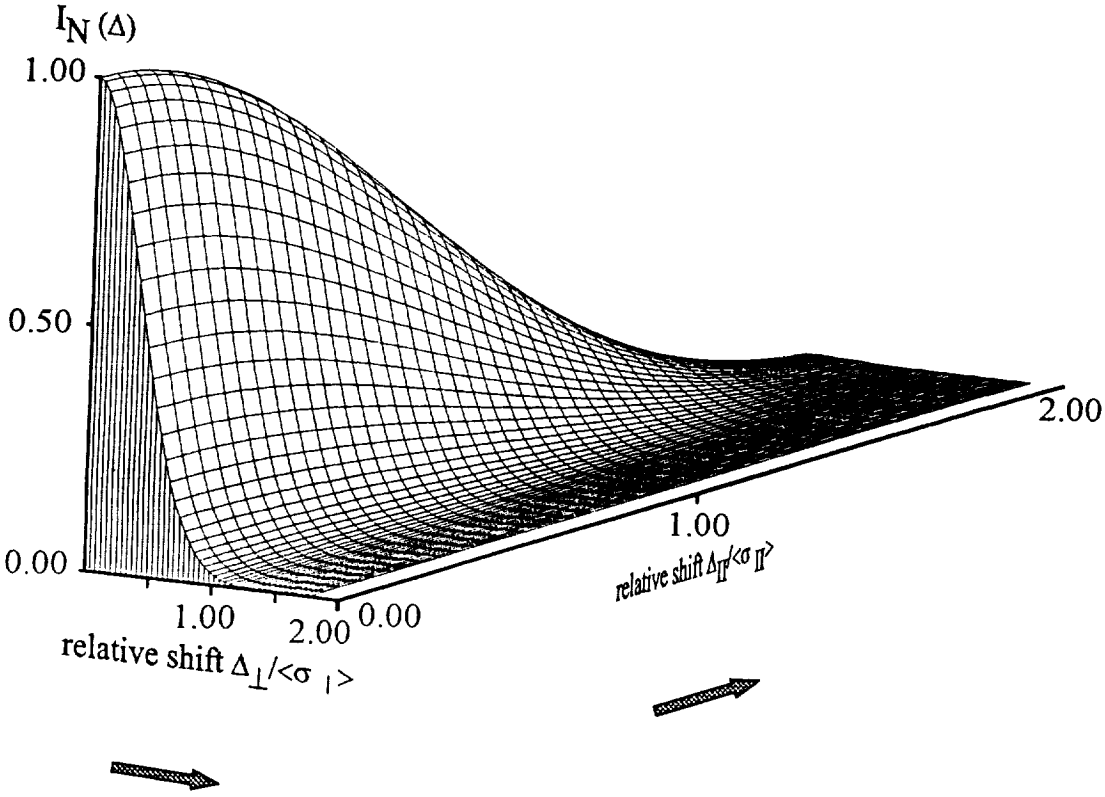
$I_N(\Delta)$
1.00
0.50
0.00
1.00
2.00
relative shift $\Delta_\perp/\langle\sigma_\perp\rangle$
0.00
1.00
2.00
relative shift $\Delta_{II}/\langle\sigma_{II}\rangle$

Fig.2

200

201

202

203

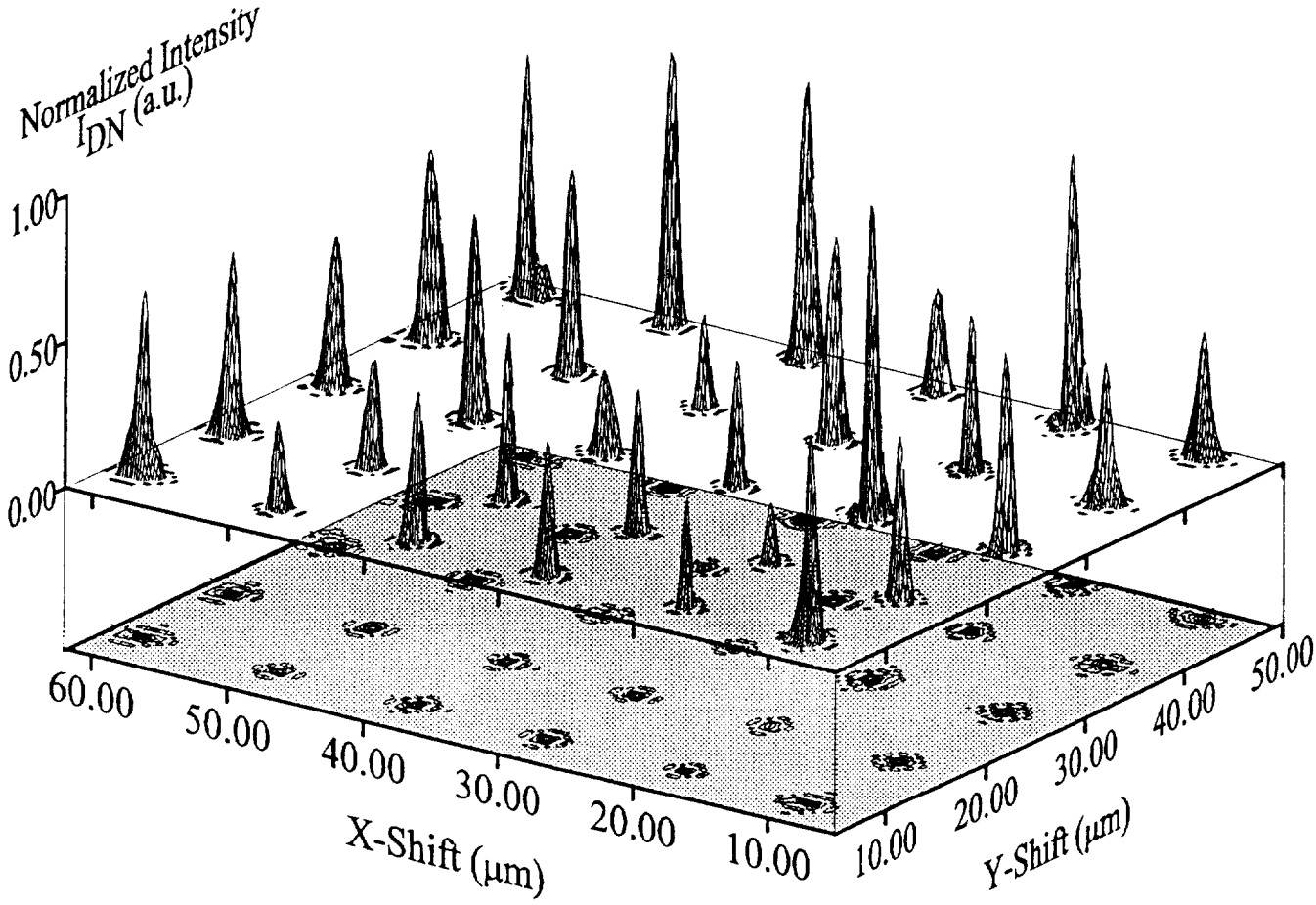

204

205

206

207

208

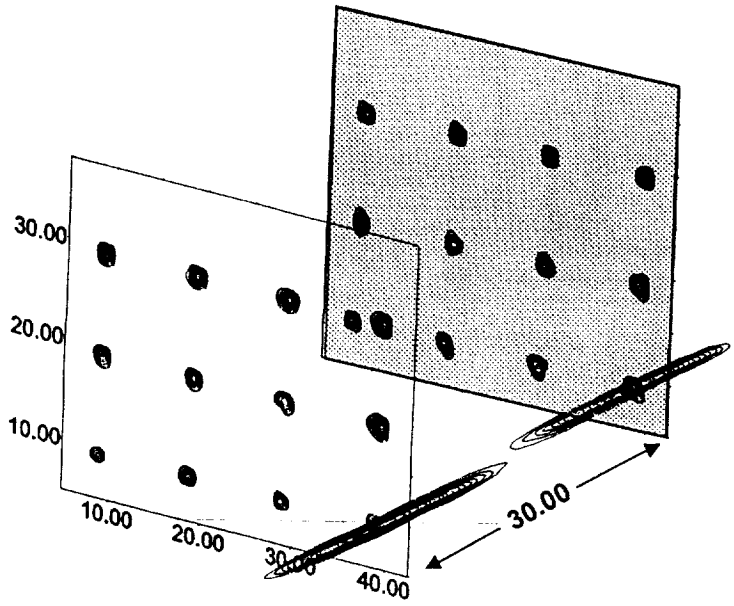
30.00
20.00
10.00
10.00
20.00
40.00
30.00